

# Poly(vinyl chloride)–Green Coconut Fiber Composites and Their Nonlinear Viscoelastic Behavior as Examined with Fourier Transform Rheometry

Jean L. Leblanc

*Polymer Rheology and Processing, University P. and M. Curie (Paris 6), LRMOP, 60 rue Auber, F-94408 Vitry-sur Seine, France*

Received 28 December 2004; accepted 22 April 2005

DOI 10.1002/app.22726

Published online in Wiley InterScience (www.interscience.wiley.com).

**ABSTRACT:** Using a purposely modified torsional dynamic rheometer with a closed cavity, I investigated composites of poly(vinyl chloride) (PVC) and green coconut fibers (GCFs) with Fourier transform (FT) rheometry, a new dynamic test technique that resolves the complex dynamic response of materials submitted to harmonic strain into their main and harmonic components. Because of instrument limitations in the low-strain region, torque signal harmonic components had to be corrected to yield results that suited established theoretical considerations. The preparation method of the composites had major effects on their linear and nonlinear viscoelastic responses; essentially, no homogeneous material could be prepared by dry blending plus extrusion, in contrast to dry blending plus mixing, which is the recommended technique; this was likely

because PVC plasticization was then achieved. One of the most important rheological characteristics of the PVC–GCF composites was the quasidisappearance of the linear viscoelastic behavior. Nevertheless, an easy extrapolation technique was used to extract linear modulus data from the FT results, which led me to the conclusion that the reinforcing effect of the GCFs was essentially hydrodynamic with little, if any, interfacial interaction between the polymer matrix and the fibers. The results gathered from nonlinear viscoelastic properties, as obtained through FT rheometry, supplement this conclusion. © 2006 Wiley Periodicals, Inc. *J Appl Polym Sci* 101: 3638–3651, 2006

**Key words:** composites; fibers; poly(vinyl chloride) (PVC); reinforcement; rheology; viscoelastic properties

## INTRODUCTION

In the coastal regions of Brazil, huge quantities of empty coconut waste are generated by the drinking of green coconut water. Such waste needs up to 10 years to disappear from dumping fields through natural degradation. Each coconut weighs approximately 700 g, and between the green thin outer shell and the central hard nut that contains the water, there is a 3–4 cm thick white and fibrous material. When this intermediate core is dried, there remain long brown fibers up to 10 cm long, which have found a number of traditional applications. It recently came to my attention that interesting composites with thermoplastic polymers could be prepared with dried green coconut fibers (GCFs) if the rheological behavior in the molten state was sufficiently understood to allow the processing techniques to be correctly monitored. Besides the obvious economical and environmental advantages that parts made out of polymer–GCF composites could offer, such complex materials present interesting challenges in terms of rheological properties, notwithstanding the basic experimental difficulties that

can be expected in the first assessment of their flow properties and, second, in the understanding of the associated polymer–fiber interactions.

Like most other complex polymer systems, polymer–GCF composites are expected to exhibit strong nonlinear viscoelastic characteristics that need special testing techniques to be studied. One such technique is Fourier transform (FT) rheometry, which was recently implemented in our laboratory, by the suitable modification of a commercial torsional dynamic rheometer (i.e., rubber process analyzer RPA 2000, Alpha Technologies) initially designed for handling highly viscous and stiff materials in the molten state, such as filled rubber compounds. Details on the modification of the rubber process analysis (RPA) for FT rheometry have been published elsewhere,<sup>1,2</sup> as have the calculation techniques to extract and analyze Fourier spectra from recorded strain ( $\gamma$ ) signals and torque signals.

The aims of this article are to present an investigation of the nonlinear viscoelastic behavior of poly(vinyl chloride) (PVC)–GCF composites with FT rheometry.

## EXPERIMENTAL

### Test materials

GCFs were supplied by Empresa Brasileira de Pesquisa Agropecuária (Rio de Janeiro, Brazil). This ma-

Correspondence to: J. L. Leblanc (jleblanc@ccr.jussieu.fr).

**TABLE I**  
**PVC-GCF Composite Samples: Formulation and Preparation Procedure**

	VCF00e2	VCF80e2	VCF70e2	VC00mi	VCF80mi	VCF70mi
PVC (wt %)	87.72	71.94	63.75	87.72	71.94	63.75
GCF (wt %)	—	17.99	27.32	—	17.99	27.32
DOP (wt %)	8.77	7.19	3.68	8.77	7.19	3.68
UBZ (wt %)	3.51	2.88	2.55	3.51	2.88	2.55
Preparation Conditions	Dry blending plus laboratory extrusion Temperature settings: (hopper) 130, 140, and 150 and (die) 160°C Screw Rotation = 60 RPM Slit die = 30 × 2 mm			Dry blending plus laboratory mixing Starting temperature: 130°C  Fill factor: 0.70 Cam rotors speed: 50 Final torque: 17–19 Nm min Dump temperature: 158–160°C		

terial results from a complex, undisclosed process, which involves the drying, grinding, and sorting of fibers from green coconut shells. The samples used in this study consisted of a mixture of a fine brown powder with dispersed yellow-orange single fibers up to 3–4 mm length; the specific gravity was 1.20 g/cm<sup>3</sup>. A standard suspension-grade PVC in powder form (Norvic SP 1100HP) was supplied by Triken-Organização Odebrecht; the specific gravity was 1.39 g/cm<sup>3</sup>.

One PVC reference formulation and two PVC-GCF composites were prepared (at the Instituto de Macromoléculas Professora Eloisa Mano, Universidade Federal do Rio de Janeiro, Brazil, in collaboration with Cristina R. G. Furtado and Leila Y. Visconte during a visit sponsored by CAPES-COFECUB.) by first dry blending the ingredients, which were then melt-mixed with a Haake Rheocord 900, fixed either with a screw extruder 3 cm in diameter or a 85-cm<sup>3</sup> mixing chamber with cam rotors. Immediately, after melt mixing, plaques around 2 mm thick were prepared by compression molding at 160°C. The formulations and preparation conditions are given in Table I. The plasticizer [dioctyl phtalate (DOP)] and the antidegradant (UBZ-790, or UBZ) were always 10 and 4 wt %, respectively, of the polymer. Table II gives the composite formulations in terms of the volume fractions of the ingredients.

### Test protocols for $\gamma$ sweep experiments

With respect to its measuring principle, the RPA cavity must be loaded with a slight volume excess of test material. In agreement with ASTM 5289, the manufacturer recommends that one load samples of around 5 g, that is, 4.4 cm<sup>3</sup>, for a standard filled rubber compound with a specific gravity of 1.14 g/cm<sup>3</sup>. With the actual dimensions of the cavity,<sup>3</sup> one calculates its near exact volume by taking into account the grooves (2 × 24 small grooves of 1 × 1.57 × 9.6 mm; the rounding of extremities is neglected) and with the central gap between upper and lower dies set equal to 0.5 mm. A theoretical cavity volume of 3280 mm<sup>3</sup> was obtained. With a volume excess of 5% used, the optimized sample loadings were 4.33, 4.27, and 4.23 g for samples VCF00, VCF80, and VCF70, respectively. Samples for RPA testing were consequently prepared by the die cutting of disks of appropriate diameter out of the molded plaques. If necessary, the samples were adjusted to maintain their weight within the optimized loading ± 0.2 g. To ensure easy filling of the RPA cavity, the samples were disposed for 2–3 min on the lower die at the test temperature (160°C) before the test chamber was closed.

$\gamma$  sweep tests were performed with RPA according to the protocols given in Table III. Each protocol describes  $\gamma$  sweep experiments through two subse-

**TABLE II**  
**PVC-GCF Composite Samples: Volume Fractions**

	VCF00e2	VCF80e2	VCF70e2	VC00mi	VCF80mi	VCF70mi
PVC	0.834	0.699	0.646	0.834	0.699	0.646
GCF	—	0.162	0.225	—	0.162	0.225
DOP	0.118	0.099	0.092	0.118	0.099	0.092
UBZ	0.048	0.040	0.037	0.048	0.040	0.037

Specific gravities: PVC = 1.39 g/cm<sup>3</sup>; GCF = 1.20 g/cm<sup>3</sup>; DOP = 0.98 g/cm<sup>3</sup>; UBZ = 0.96 g/cm<sup>3</sup>.

**TABLE III**  
**RPA  $\gamma$  Sweep Test Protocols**

Test protocol					
Ssweep_1Hz_A			Ssweep_1Hz_B		
$\gamma$ sweep (run 1) $\gamma$ ( $^{\circ}$ )	Dwell time	$\gamma$ sweep (run 2) $\gamma$ ( $^{\circ}$ )	$\gamma$ sweep (run 1) $\gamma$ ( $^{\circ}$ )	Dwell time	$\gamma$ sweep (run 2) $\gamma$ ( $^{\circ}$ )
	2 min at rest			2 min at rest	
0.5		0.6	0.6		0.5
1.0		1.5	1.5		1.0
2.5		3.5	3.5		2.5
5.0		6.7	6.7		5.0
8.5		10.0	10.0		8.5
12.0		14.5	14.5		12.0
17.0		20.0	20.0		17.0
22.5		25.0	25.0		22.5
27.5		30.0	30.0		27.5
31.5		33.0	33.0		31.5

RPA test conditions: temperature as selected; frequency = 1 Hz. Sample conditioning: preheating = 3 min at rest; Fixing = 30 s, 1 Hz, and 20 $^{\circ}$ ; preheating = 2 min at rest.

quent runs separated by a resting period of 2 min. At least two samples of the same material were tested, with the protocols named Ssweep\_1Hz\_A and Ssweep\_1Hz\_B, such that through the inversion of the  $\gamma$  sequences (i.e., run 1 and run 2), sample fatigue effects, if any, would be detected. At each  $\gamma$  sweep step, data acquisition (with a technique described elsewhere<sup>1</sup>) was made to record 10,240 points at the rate of 512 points/s. Twenty cycles were consequently recorded at each  $\gamma$  step, with the RPA set to apply a sufficient number of cycles (i.e., 40 cycles; the stability condition) for the steady harmonic regime to be reached. Data acquisition was activated as soon as the RPA test-monitoring screen had informed the operator that the set  $\gamma$  was reached and was apparently stable.

With the protocols described in Table III, two subsequent  $\gamma$  sweep tests were performed within the limits of the instrument at the frequency considered to capture signals up to the far nonlinear region with evidence, if any, for the  $\gamma$  sensitivity of the material. Each experiment lasted some 23 min, and two samples were tested with the two protocols in such a manner that the  $\gamma$  sequences of the successive runs were inverted. The  $\gamma$  range was documented by 20 experimental points, and any differences between runs 1 and 2 indicated that the tested material was sensitive to  $\gamma$  amplitude. This experimental procedure was designed to obtain the maximum number of data in the shortest test time (<1 h), with documentation in the meantime of the test repeatability and the material homogeneity.

## FT analysis

The modified RPA yielded both  $\gamma$  signals and torque signals as recorded data files of actual harmonic  $\gamma$  and stress readings versus time. As previously described,<sup>2</sup> conditions for optimal data capture were as follows. First, the actual test conditions in terms of temperature, frequency, and  $\gamma$  angle were selected through built-in capabilities; then, the sample was positioned on the lower die, and the cavity was closed. The test was started, and the data-acquisition system was activated to record at each  $\gamma$  step the selected number of data points with respect to the acquisition parameters used (i.e., 10,240 points at 512 points/s in this study).

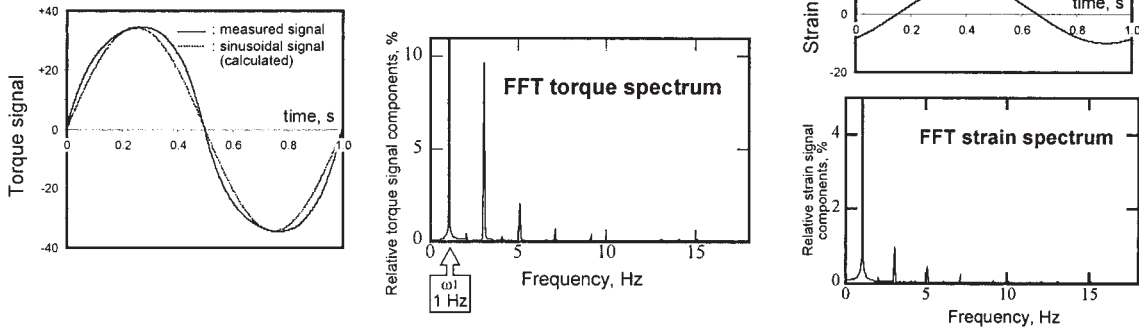
A specific calculation program, written with the FT algorithm available in MathCad 8.0 (MathSoft, Inc.) was used to obtain the amplitude of the main stress and  $\gamma$  components (corresponding to the test frequency) and the relative magnitudes (%) of the odd harmonic components, that is,  $I(n\omega_1)/I(\omega_1)$  [where  $I(n\omega_1)/I(\omega_1)$ , or the abridged form  $I(n/1)$ , is used to describe the  $n$ th relative harmonic component of any harmonic signal;  $S(n\omega_1)/S(\omega_1)$ , or  $S(n/1)$ , specifically means that a  $\gamma$  signal is considered; and  $T(n\omega_1)/T(\omega_1)$ , or  $T(n/1)$  is used for the torque signal]. The number of data points used, the frequency resolution (Hz), the acquisition time (s), and the sampling rate (points/s) were also provided. Figure 1 shows the average torque signals and  $\gamma$  signals (averaged from 20 recorded cycles, i.e., 10,240 data points) observed when a PVC-GCF composite (i.e., sample VCF70e2) was submitted to a 10 $^{\circ}$   $\gamma$  at 1 Hz. As shown, both signals were harmonic, but the torque one was distorted in comparison with a sinusoid of the same amplitude. The single FT spectra obtained through calculation on the last 8192 points of the recorded signals are shown, and as also shown, the torque FT spectrum (the middle in the figure) exhibited significant third and fifth harmonics with further ones becoming very small. The results of the odd harmonic components analysis on both the torque signals and  $\gamma$  signals are displayed in the inserted table. The very low  $\gamma$  harmonic peaks (<1%) indicated the excellent quality of the applied signal, at least at this  $\gamma$  angle (10 $^{\circ}$ ).

## RESULTS AND DISCUSSION

### Harmonic $\gamma$ signal quality

In dynamic testing, a perfect sinusoidal deformation at a controlled frequency and  $\gamma$  should ideally be applied on the test material. In the RPA, the (harmonic)  $\gamma$  on the material occurs by means of an oscillating wall, that is, the lower die, through the monitored operation of a high-precision motor. As

PVC cpd ( $\Phi_{GCF} = 0.225$ ) ; 10.0 deg; 1 Hz; 160°C



Fourier transform spectra; odd harmonic components analysis

Nr points	Freq.resol.	Main freq.	3 <sup>rd</sup> harm.	5 <sup>th</sup> harm.	7 <sup>th</sup> harm.	9 <sup>th</sup> harm.	11 <sup>th</sup> harm.	13 <sup>th</sup> harm.	15 <sup>th</sup> harm.
$t_{aq}$	Sampling pt/s	Main Torq. a.u.	$T(3\omega_1)/T(\omega_1)$ %	$T(5\omega_1)/T(\omega_1)$ %	$T(7\omega_1)/T(\omega_1)$ %	$T(9\omega_1)/T(\omega_1)$ %	$T(11\omega_1)/T(\omega_1)$ %	$T(13\omega_1)/T(\omega_1)$ %	$T(15\omega_1)/T(\omega_1)$ %
		Main Strain a.u.	$S(3\omega_1)/S(\omega_1)$ %	$S(5\omega_1)/S(\omega_1)$ %	$S(7\omega_1)/S(\omega_1)$ %	$S(9\omega_1)/S(\omega_1)$ %	$S(11\omega_1)/S(\omega_1)$ %	$S(13\omega_1)/S(\omega_1)$ %	$S(15\omega_1)/S(\omega_1)$ %
8192	0.063	<b>1</b>	3	5	7	9	11	13	15
16.0	512	<b>1691.0</b>	9.707	2.029	0.674	0.250	0.046	0.090	0.093
		<b>455.5</b>	0.954	0.432	0.152	0.055	0.017	0.024	0.022

Figure 1 Typical FT rheometry results on a PVC-GCF composite.

previously reported, RPA meets technical limits in accurately producing the harmonic mechanical motion, as with any other test devices. Fast FT of the  $\gamma$  (i.e., applied) signal allows this aspect to be accurately documented, and whatever the material tested, two aspects are worth underlining, as illustrated in Figure 2. First, a linear relationship was observed between the set  $\gamma$  angle and the main  $\gamma$  component (in arbitrary units), which meant that in terms of  $\gamma$  crest signal, the maximum oscillation angle of the lower die could be considered as nearly perfect. Second, at a low angle, there were signifi-

cant odd harmonics in the  $\gamma$  signal, whose magnitude decreased as  $\gamma$  amplitude increased. As shown in the right part of Figure 2, the relative third harmonic  $\gamma$  component (the largest one) passed below 1% when the  $\gamma$  angle was higher than 8–10° when either the unfilled PVC or a PVC-GCF formulation was tested. The bold curve corresponds to similar data obtained when the cavity was empty and further demonstrated that loading the cavity significantly decreased the  $\gamma$  signal quality, as previously investigated in detail.<sup>3</sup> The actual stiffness of the tested material thus had a slight but significant ef-

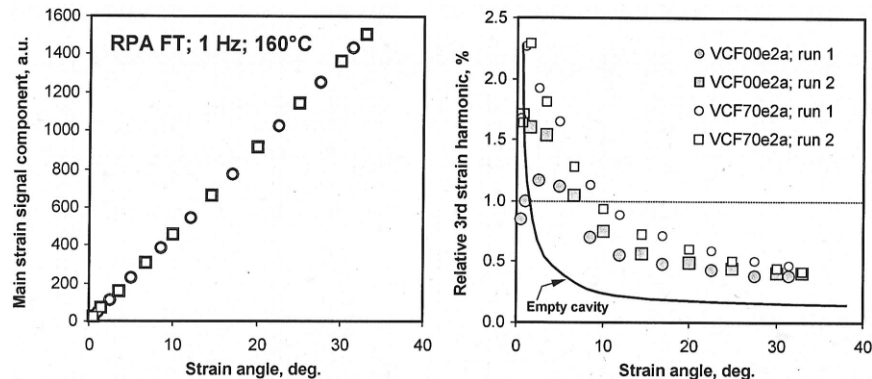


Figure 2 Applied  $\gamma$  signal quality; the bold curve in the right part of the figure was drawn with a simple three-parameter hyperbolic decay equation, that is,  $S(3/1) = a + (bc/c + \gamma)$ , where  $a = 0.086$ ,  $b = 4.31$ , and  $c = 0.408$ . See ref. 3 for details.

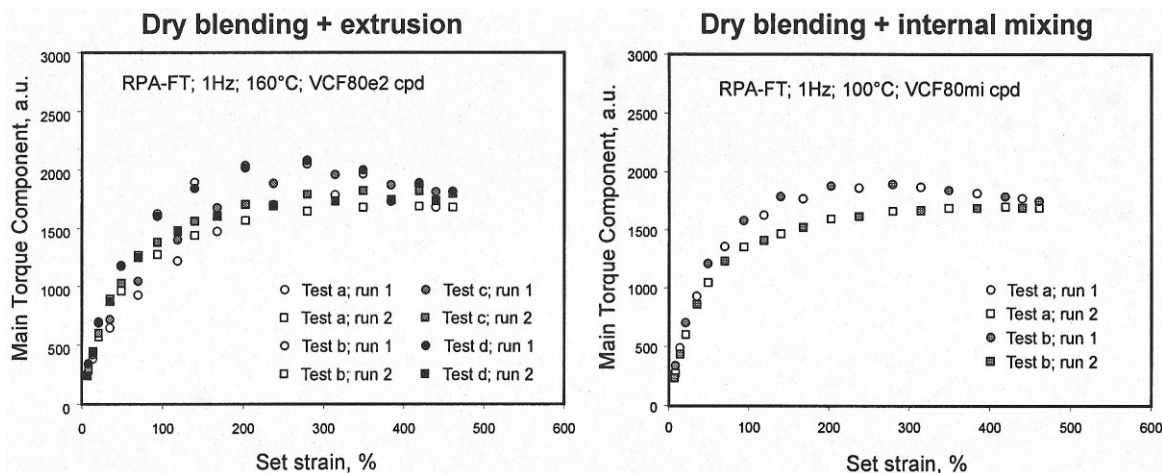


Figure 3 Effect of the sample preparation technique on the dynamic properties.

fect, which, however, decreased as the  $\gamma$  angle increased in such a manner that the nonlinear viscoelastic region (i.e., at a high  $\gamma$  angle) could be investigated in confidence.

### Main torque component

The results obtained for the main torque components  $T(\omega_1)$  of two samples of the same test material did not superimpose well when dry blending plus extrusion was used in contrast with dry blending plus mixing, which resulted in excellent homogeneity. To further document the poor sample homogeneity when simple extrusion was used, additional tests were made with more samples. Figure 3 compares, for instance, the two preparation techniques in the case of a PVC–GCF composite. The large scatter seen on the left graph clearly demonstrates that dry blending plus extrusion did not lead to good sample homogeneity. When internal mixing (right graph) was used, the samples were homogeneous, as reflected by the excellent superposition of data when two samples (tests a and b) were tested; a significant difference was also seen between runs 1 and 2, which is discussed later.

The lack of sample homogeneity when extrusion was used was also observed with the unfilled PVC composition. This, of course, suggests that it was a defect in PVC plasticization rather than in the fiber dispersion that was responsible for the observed experimental scatter.

Whatever the sample,  $T(\omega_1)$  versus set  $\gamma$  curves revealed that after an initial very short linear region [i.e.,  $T(\omega_1)$  was directly proportional to  $\gamma$ ], the materials exhibited a strong nonlinearity. The ratio  $T(\omega_1)/\gamma$  obviously had the meaning of a modulus and, with respect to the data-acquisition conditions used for FT calculation, was converted to complex

modulus ( $G^*$ ) with the following equality:  $G^*$  (kPa) =  $12.335T(\omega_1)/\gamma$  [where  $T(\omega_1)$  is in arbitrary units and  $\gamma$  in %]. As shown in Figure 4, for the unfilled PVC composition,  $G^*$  versus  $\gamma$  curves yielded a more familiar picture of a plateau region at low strain than a typical  $\gamma$  dependence. Although the large scatter did not permit easy observation with samples prepared by extrusion, there was a significant difference between the data gathered between runs 1 and 2, which suggested that the material was somewhat sensitive to  $\gamma$  history.

With reference to the mathematical form of the so-called Cross equation for the shear viscosity function, such a behavior was adequately modeled with

$$G^*(\gamma) = G_0^* \left[ \frac{1}{1 + (A\gamma)^B} \right] \quad (1)$$

where  $G_0^*$  is the modulus in the linear region,  $A$  is the reverse of a critical strain at which half the linear modulus is reached, and  $B$  is a parameter describing the strain sensitivity of the material, as illustrated in Figure 5. The so-derived  $G_0^*$  was obviously the initial slope of  $T(\omega_1)$  versus  $\gamma$ .

Table IV gives the fit parameters of eq. (1) for all of the materials tested; the reverse of parameter  $A$  is given. As shown,  $G_0^*$  was systematically lower for the second run, and the higher the fiber content was, the larger the difference was, as illustrated when the lower left graph in Figure 3 is compared with Figure 6, drawn with data obtained from the PVC–GCF compositions prepared by internal mixing.

Figure 6 shows that within the experimental  $\gamma$  window permitted by the RPA, the filled PVC composites did not exhibit a linear behavior. This means that with a standard dynamic testing technique, measurements

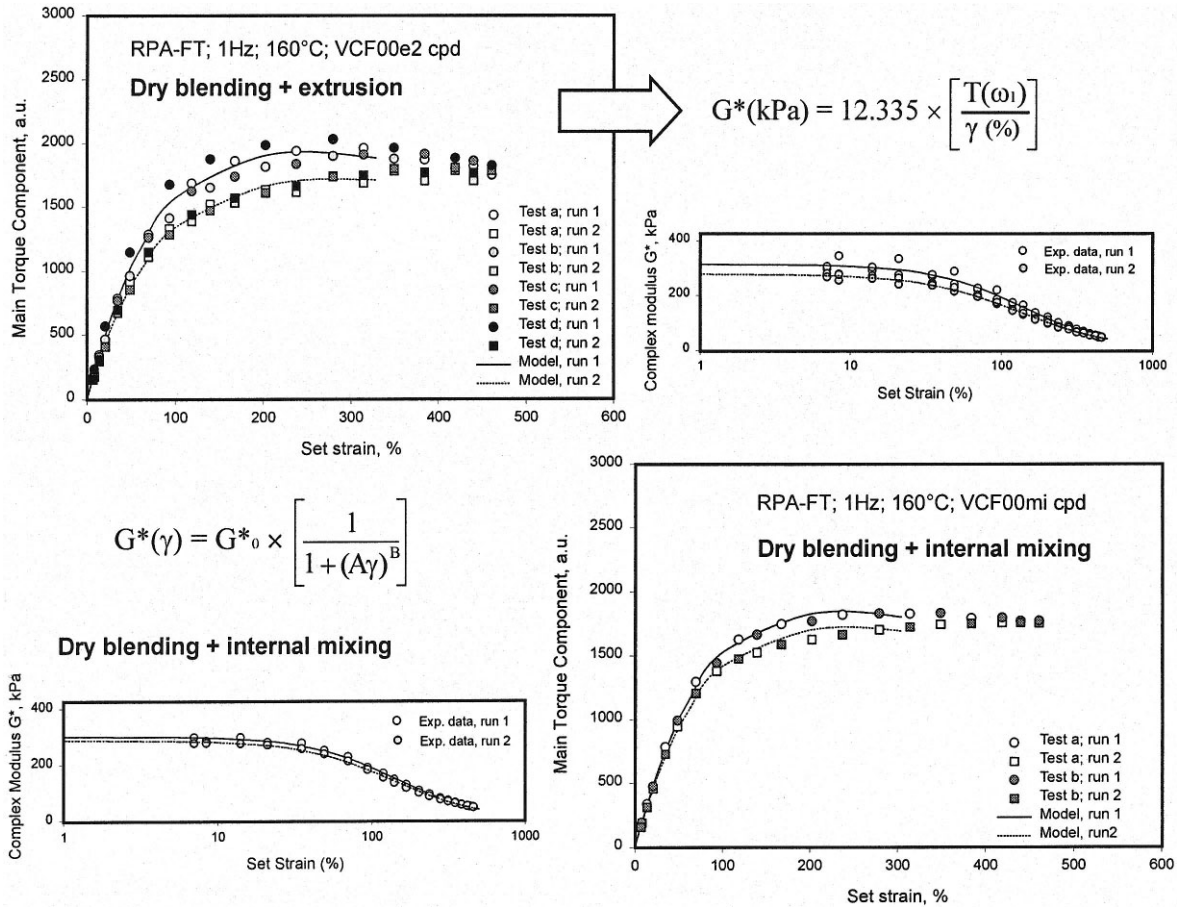


**Figure 4** Main torque component variation with set  $\gamma$  of unfilled PVC formulations prepared by either extrusion or internal mixing.

made in such conditions would be at best apparent because the stress- $\gamma$  proportionality was no longer met. The advantages of FT rheometry in the case of complex polymer systems appeared thus here. Indeed,

by resolving the measured torque signal into its main component, I had access to  $G^*$ , which was fitted with eq. (1) to yield  $G_0^*$ . This quantity accounts for the net effect of filler loading independently of the structural damages due to the amplitude of the applied  $\gamma$ . As shown in Figure 7, the reinforcing effect of the GCFs

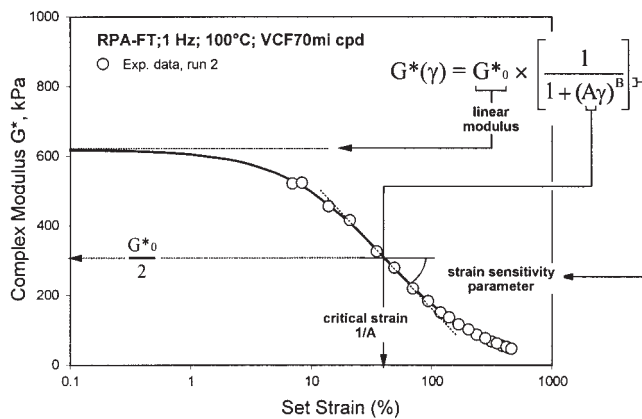


**Figure 5** Modeled variation of the dynamic modulus with  $\gamma$  amplitude (the data is on the 27% GCF composition prepared by internal mixing)

**TABLE IV**  
 **$G^*$  Versus  $\gamma$ : Fitting Parameters for Eq. (2)**

Sample	Run	$G_0^*$ (kPa)	$1/A$ (%)	$B$	$r^2$
VCF00e2	1	314.2	139.7	1.44	0.9817
VCF00e2	2	278.6	133.2	1.33	0.9958
VCF00mi	1	302.0	140.6	1.48	0.9975
VCF00mi	2	287.5	136.1	1.44	0.9978
VCF80e2	1	571.8	38.0	0.88	0.9529
VCF80e2	2	473.8	58.8	1.07	0.9977
VCF80mi	1	534.9	59.5	1.10	0.9976
VCF80mi	2	449.2	65.8	1.15	0.9997
VCF70e2	1	1160.7	22.0	0.92	0.9869
VCF70e2	2	704.7	35.9	0.98	0.9969
VCF70mi	1	798.6	34.7	0.99	0.9991
VCF70mi	2	619.6	39.9	1.02	0.9994

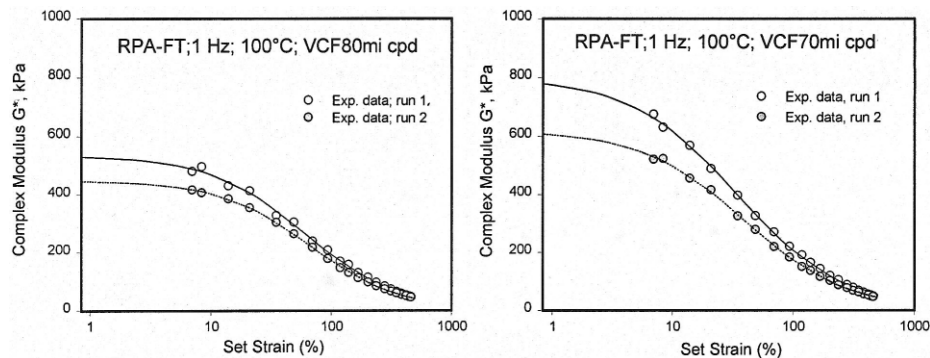


**Figure 6** Modeled variation of the dynamic modulus with  $\gamma$  amplitude and the effect of fiber content and shear history (i.e., run 1 vs. run 2). The compounds were prepared by internal mixing.

was clearly detected when  $G_0^*$  versus the fiber volume fraction was plotted.

It is tempting to consider the GCF loading effect with respect to well-known models, such as the Guth–Gold–Simha equation:<sup>4,5</sup>

$$G_{\text{cpd}} = G_0(1 + 2.5\Phi + 14.1\Phi^2) \quad (2)$$

The dashed line drawn in Figure 7 corresponds to eq. (2) with  $G_0 = 314.2 \pm 15.7$ , that is, the mean values measured on the unfilled PVC compositions. As shown, the measured data of the PVC–GCF composites were slightly below the model, except one datum, which suffered from a large experimental scatter. In developing their model, Guth, Gold, and Simha considered suspensions of spheres of equal diameter, to which they assigned a pure hydrodynamic effect. Consequently, their model is expected to fail when there are physicochemical interactions between the matrix and the dispersed phase, as indeed reported by

many authors. Conversely, one could consider that the closer to the model are the experimental data, the less probable polymer–filler interactions are. It follows that data in Figure 7 strongly suggest that there were no significant interactions between the PVC matrix and the GCFs.

Parameters  $A$  (or  $1/A$ ) and  $B$  in eq. (1) are concerned with the  $\gamma$  sensitivity of materials. As shown in the left graph of Figure 8, the higher the fiber content was, the shorter the linear viscoelastic region was because  $1/A$  corresponded to a  $\gamma$  magnitude at which half  $G_0^*$  was measured. The parameter  $B$  expresses the sensitivity of the material to  $\gamma$  amplitude; with respect to eq. (1), the smaller  $B$  is, the more severe the modulus drop is. The variation of both  $1/A$  and  $B$  with fiber volume fraction was essentially linear, with no significant effect of  $\gamma$  history (i.e., runs 1 and 2 gave the same results) or preparation technique, when I took into account the poor plasticization of PVC in the extruder and, hence, the resulting material inhomogeneity.

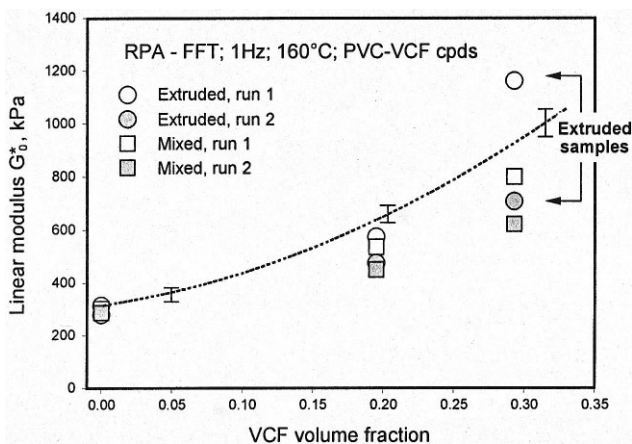


**Figure 7** Effect of filler loading and preparation mode on the (extrapolated) linear dynamic modulus of PVC–GCF composites; the dashed line represents data calculated with the Guth–Gold model.

### Torque harmonic components analysis

Through FT on 8192 ( $2^{13}$ ) data points, harmonics up to  $T(15\omega_1)$  or higher were detected, whereas above the fifth one, they became too small to be unambiguously distinguished from the noise. The limit of the relative torque harmonic  $T(n\omega_1)/T(\omega_1)$  [or  $T(n/1)$ ] was expected to be equal to  $1/n$ , and  $T(3/1)$  was consequently the most intense contribution compared to all of the other harmonics. The relative third torque harmonic component was, therefore, the most interesting data for nonlinear viscoelastic characterization.

As previously reported for various polymer systems, either pure or unfilled materials,<sup>2,3</sup> the variation of the relative third torque harmonic component with the  $\gamma$  amplitude is generally such that an S-shaped curve is observed, from a (scattered) plateau value at low  $\gamma$  up to a maximum at high  $\gamma$ . Figure 9 shows this behavior in the case of the unfilled PVC compounds

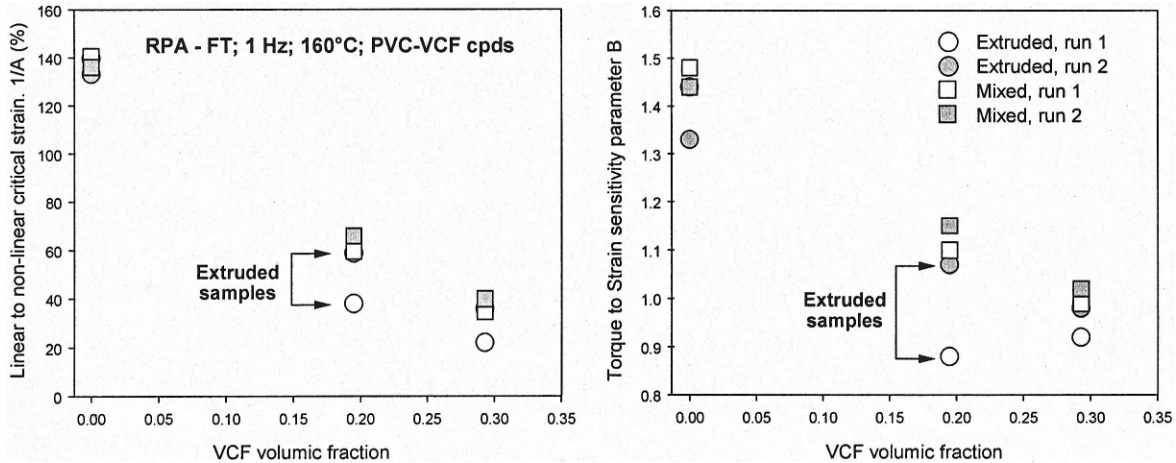


Figure 8 Effect of fiber content on the  $\gamma$  sensitivity of the PVC-GCF composites

prepared by mixing. A similar figure was obtained with samples prepared by extrusion, but a large scatter was observed, which essentially reflected material inhomogeneity. Because, except for experimental scatter, samples prepared either by extrusion or mixing exhibited qualitatively and quantitatively the same behavior, only results with composites prepared by mixing are discussed hereafter. As shown in Figure 9, no significant  $\gamma$  history effect was detected for unfilled PVC because the data for runs 1 and 2 superimposed well; in addition, the material was very homogeneous because no difference was seen between tests a and b. At low  $\gamma$ , the data were somewhat scattered, as shown by the insert, where magnification was obtained with logarithmic scales.

The scatter at low  $\gamma$  was attributed to the deteriorating quality of the  $\gamma$  signal as the deformation angle

decreased, as discussed previously. The simultaneous treatment of torque and  $\gamma$  signals through FT gave access to both  $T(n/1)$  and  $S(n/1)$ . As previously discussed in detail,<sup>2</sup>  $T(3/1)$  data that do not mainly express the nonlinearity of the material itself can be excluded from any analysis of the nonlinear behavior of a material with an appropriate exclusion criterion. Although relatively successful, this  $T(3/1)$  data treatment technique nevertheless left nonzero harmonics as  $\gamma$  decreased to zero, in contradiction with theoretical expectations. A fortuitous observation suggested to us recently a most effective correction method for instrumental deficiencies at low  $\gamma$ .

As demonstrated in an earlier section, fast FT of the  $\gamma$  (i.e., applied) signal allowed the quality of the applied  $\gamma$  signal to be precisely documented, for instance, by consideration of the relative third harmonic  $\gamma$  component, that is,  $S(3/1)$ , which decreased as  $\gamma$  amplitude increased, whatever the test conditions, and generally passes below 1% of the main component when the  $\gamma$  angle was higher than 1.3–1.5° (see Fig. 10, upper left graph). In other terms, high  $\gamma$  tests performed in better-applied signal conditions than low  $\gamma$  ones. A plot of  $T(3/1)$  versus  $S(3/1)$  suggested, however, an adequate method to correct the third torque harmonic component for deficiencies in applied  $\gamma$ . As shown in the right graph of Figure 10,  $T(3/1)$  versus  $S(3/1)$  decreased, passed through a minimum, and appeared to be bounded by a straight line whose slope was a multiple of  $\frac{1}{3}$ . If an ideal elastic material, for instance, the calibration spring, was tested, the slope was  $\frac{2}{3}$ . The correction method was based on the simple argument that if the applied  $\gamma$  were perfect, all  $T(3/1)$  data points would fall on the vertical axis. Consequently, the  $T(3/1)$  data were corrected according to

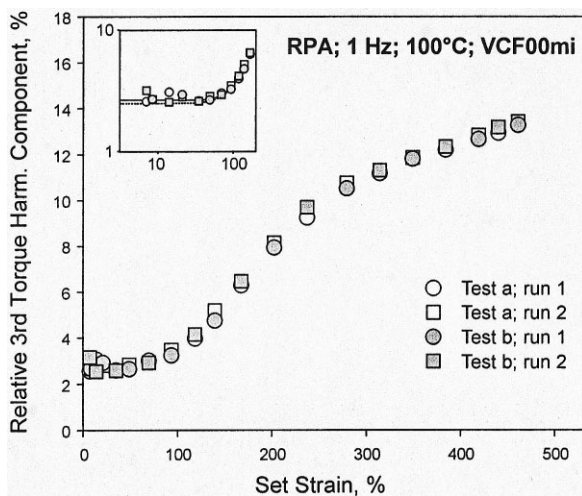


Figure 9 Relative third torque harmonic versus  $\gamma$  for the unfilled PVC compound prepared by dry blending plus mixing; two samples were tested.

$$T(3/1)_{\text{corr}} = T(3/1)_{\text{TF}} - \frac{CF}{3} S(3/1)_{\text{TF}} \quad (3)$$



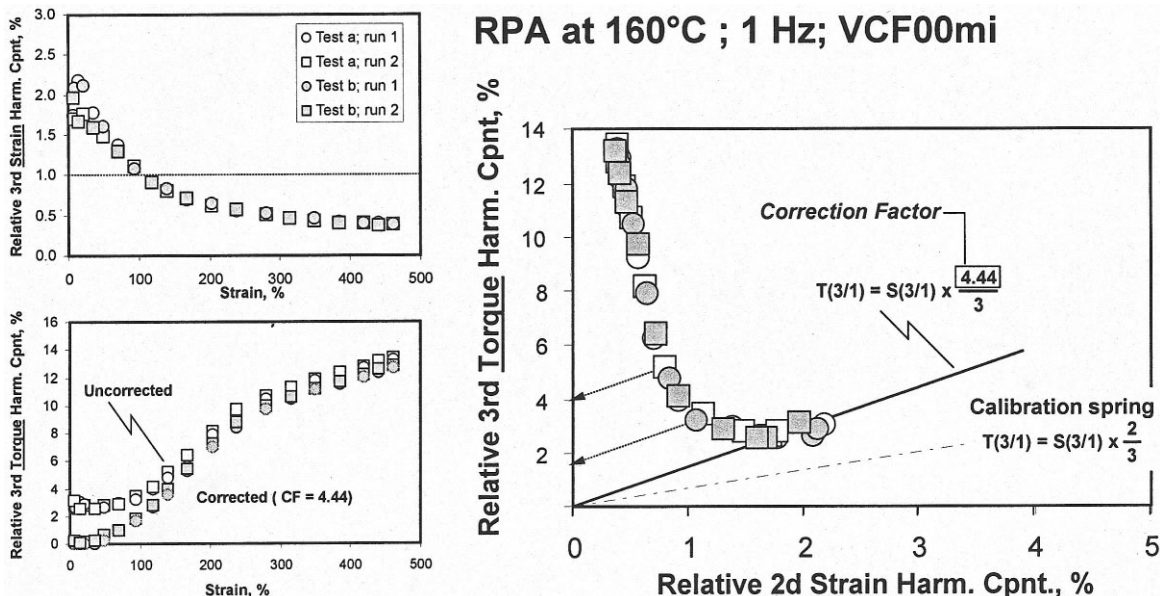


Figure 10 Correction method on the third relative torque component data.

where  $T(3/1)_{TF}$  and  $S(3/1)_{TF}$  are the third relative harmonic components of the torque and strain signals, respectively, and CF is the correction factor as derived from the  $T(3/1)$  versus  $S(3/1)$  plot. The lower left graph in Figure 10 shows how this correction method works, with the immediate result that at low  $\gamma$ , when the viscoelastic response of the material was expected to be linear, the corrected third relative torque harmonic component vanished, in agreement with theory.<sup>6</sup>

The typical S-shaped variation of  $\gamma$  of corrected  $T(3/1)$  is shown in Figure 10 for the unfilled PVC compound. Similar plots were obtained with the GCF-filled materials, with some differences im-

parted by fiber loading; essentially, the higher the fiber content was, the steeper the curve was and the higher the limiting value was at high  $\gamma$  (Fig. 11). Also, the initial flat region at low  $\gamma$ , where  $T(3/1)$  went to zero, was larger with the unfilled material and tended to disappear as the fiber content increased.

At low  $\gamma$ ,  $T(3/1)$  vanished when it was corrected for applied signal deficiencies. Consequently, the simple equation used in previous publications<sup>2,3</sup> to model the observed  $T(3/1)$  behavior, had to be modified to consider a variation from zero at low strain toward a maximum plateau value at high (infinite) strain [ $T(3/1)_{max}$ ] according to

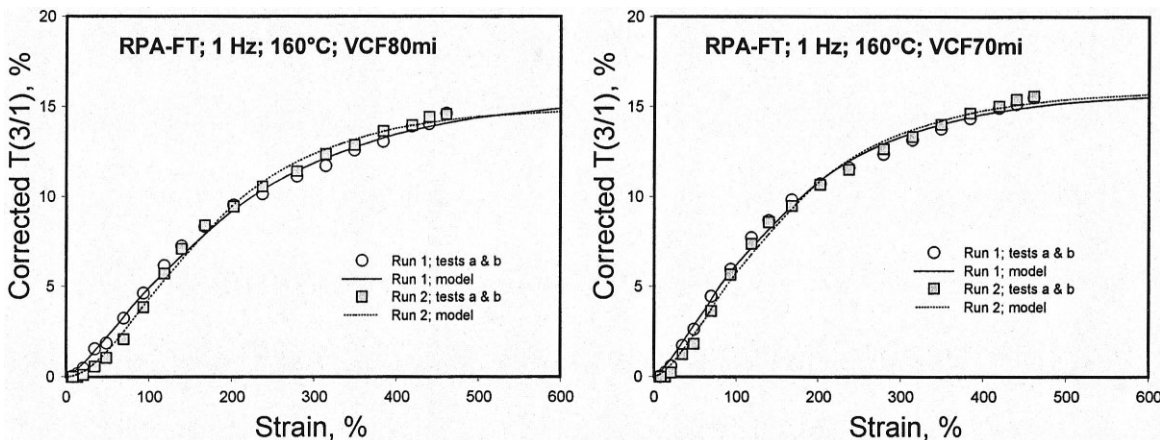


Figure 11 Corrected relative third torque harmonic versus  $\gamma$  for the PVC-GCF composites prepared by dry blending plus mixing; two samples were tested.

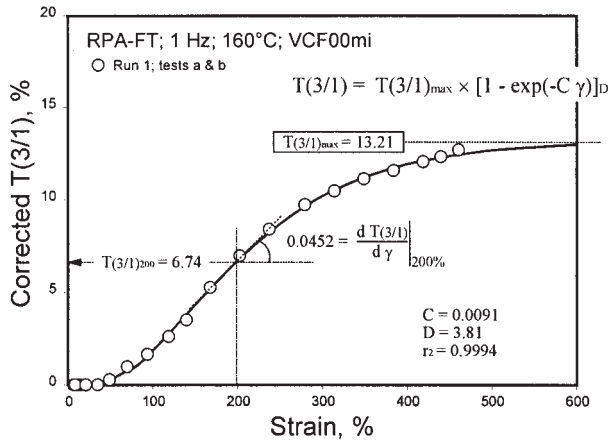


Figure 12 Modeling of  $T(3/1)$  variation with increasing  $\gamma$ .

$$T(3/1)_\gamma = T(3/1)_{\max} [1 - \exp(-C\gamma)]^D \quad (4)$$

where  $\gamma$  is the deformation or strain (%) and  $C$  and  $D$  are fit parameters. [When using eq. (4) to model  $T(3/1)$  variation with  $\gamma$ , one may express  $\gamma$  either in angle degrees or as a percentage. Obviously, all parameters remain the same except  $C$ , whose value depends on the unit for  $\gamma$ . The following equality applied for the conversion:  $C(\gamma, ^\circ) = 180\alpha/100\pi \times C(\gamma, \%)$ , where  $\alpha = 0.125$  rad.] Figure 12 illustrates how the model fit the measured data for the unfilled PVC compound prepared by blending plus mixing and shows typical features that could be derived when the data was fitted.

Table V gives the fit parameters of eq. (4) for all of the materials tested. The correlation coefficients were excellent. The values of the limiting harmonic  $T(3/1)_{\max}$  had relatively little meaning in the experimental context because the maximum permitted  $\gamma$  ( $33^\circ$  or  $461\%$ ) at 1 Hz gave access to experimental data that were far from the plateau at infinite  $\gamma$ . However, when  $T(3/1)$  versus  $\gamma$  plots for the PVC-GCF composites (Fig. 11) were considered, there was no doubt that the  $T(3/1)_{\max}$  plateau existed, and it has been clearly seen elsewhere when testing other materials, either gum EPDMs<sup>2</sup> or gum SBRs.<sup>7</sup> The data in Table V tended to show that  $T(3/1)_{\max}$  increased with higher GCF loading. With respect to nonlinear viscoelastic behavior, the most significant information, however, was provided by parameters  $C$  and  $D$ , which quantified the  $\gamma$  sensitivity of the materials.

Analysis of the  $\gamma$  sensitivity through two parameters, which somehow depended on each other, was nevertheless complicated. I circumvented this difficulty by considering the first derivative of eq. (4) to

calculate the slope of  $T(3/1)$  versus  $\gamma$  curves at any  $\gamma$ , as follows

$$S_p(\gamma) = \frac{dT(3/1)}{d\gamma} = T(3/1)_{\max} CD \exp(-C\gamma) [1 - \exp(-C\gamma)]^{D-1} \quad (5)$$

Slopes at  $\gamma = 20\%$  and  $T(3/1)$  at the same  $\gamma$ , as calculated for all samples, are given in Table VI, with respect to GCF volume fraction. As can be seen, the preparation mode (i.e., dry blending and either extrusion or mixing) and  $\gamma$  history had marginal effects (i.e., there was no significant difference between runs 1 and 2). Mean values were consequently calculated, which clearly showed that the relative third harmonic torque component increased with GCF content, whereas the slope at  $200\%$   $\gamma$  decreased with higher fiber content.

Figure 13 summarizes in graphical form the conclusions drawn from the data given in Table V. The curves were fit to experimental data with eq. (4). As shown, the main effect arose from fiber loading, and no significant difference was seen between runs 1 and 2. There was indeed a slight variation of the slope at  $200\%$  with fiber content, but the most obvious effect was the quasidisappearance of any linear response in the low  $\gamma$  region. The unfilled PVC compound (VCF00mi) still exhibited near zero  $T(3/1)$  values until  $70\text{--}80\%$   $\gamma$  was reached, in contrast with the fiber-loaded composites, whose torque response had significant third (and higher) harmonic components at the lowest  $\gamma$  investigated.

TABLE V  
Modelling of the Variation of the Third Relative Torque Harmonic with Strain: Fit Parameters of Eq. (4)

Test	Model: $T(3/1)_\gamma = T(3/1)_{\max} \times [1 - \exp(-C\gamma)]^D$			
	$T(3/1)_{\max}$	$C$	$D$	$r^2$
VCF00e2, run 1	12.71	0.0076	2.93	0.9981
VCF00e2, run 2	13.21	0.0076	2.57	0.9978
VCF00mi, run 1	13.21	0.0091	3.81	0.9994
VCF00mi, run 2	13.45	0.0088	3.45	0.9988
VCF80e2, run 1	15.73	0.0040	0.95	0.9724
VCF80e2, run 2	14.75	0.0072	1.81	0.9946
VCF80mi, run 1	15.58	0.0058	1.41	0.9971
VCF80mi, run 2	14.95	0.0083	2.18	0.9974
VCF70e2, run 1	15.45	0.0063	1.22	0.9952
VCF70e2, run 2	15.54	0.0078	1.61	0.9964
VCF70mi, run 1	15.83	0.0072	1.41	0.9966
VCF70mi, run 2	15.93	0.0079	1.69	0.9967

**TABLE VI**  
**Effect of GCF Loading on the Nonlinear Viscoelastic Parameters of the PVC–GCF Composites as Obtained Through Rheometry**

Test sample	$\Phi_{\text{GCF}}$	$T(3/1)$ at $\gamma = 200\%$		Slope at $\gamma = 200\%$	
VCF00e2, run 1	0.0	6.17	$6.17 \pm 0.40$	0.0384	$0.0384 \pm 0.004$
VCF00e2, run 2		7.01		0.0383	
VCF00mi, run 1		6.74		0.0452	
VCF00mi, run 2	0.162	7.01	$8.92 \pm 0.22$	0.0442	$0.0277 \pm 0.005$
VCF80e2, run 1		8.92		0.0277	
VCF80e2, run 2		9.04		0.0366	
VCF80mi, run 1	0.225	9.17	$10.28 \pm 0.25$	0.0342	$0.0313 \pm 0.003$
VCF80mi, run 2		9.44		0.0401	
VCF70e2, run 1		10.28		0.0313	
VCF70e2, run 2	10.63	10.63	10.63	0.0355	10.63
VCF70mi, run 1		10.81		0.0341	
VCF70mi, run 2		10.79		0.0374	

$T(3/1)|_{200\%}$  and  $dT(3/1)/d\gamma_{200\%}$  were calculated with eqs. (4) and (5).

## CONCLUSIONS

FT rheometry is a very fast and accurate technique for investigating the nonlinear viscoelastic behavior of complex polymer systems, namely, PVC–GCF composites. Adequate  $\gamma$  sweep test protocols lead to reproducible results, particularly in the high  $\gamma$  region, thanks to the closed-test-cavity design of RPA purposely modified for FT experiments. Appropriate data treatment allows minor instrument deficiencies to be compensated for to yield meaningful results in line with theoretical expectations.

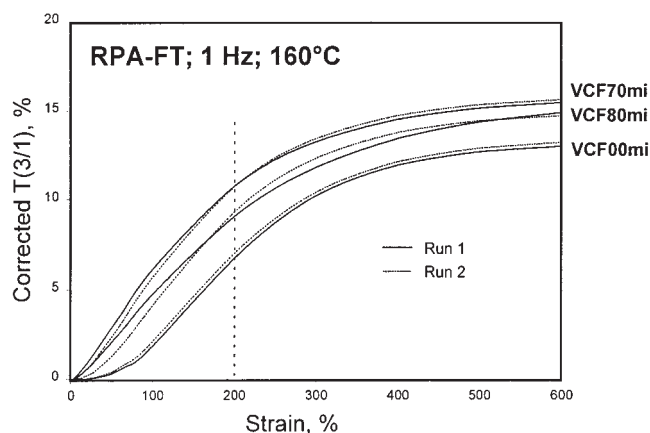


**Figure 13** PVC–GCF composites prepared by dry blending plus mixing and the effect of GCF loading on the corrected relative third torque harmonic component; the vertical dashed lines indicate the  $\gamma$  at which the results given in Table VI were calculated with eqs. (4) and (5).

As such, FT spectra contain all the information available through harmonic testing, without any conditions, as is the case with linear dynamic testing, which requires insensitivity of the modulus on  $\gamma$  amplitude. A basic analysis of the nonlinear viscoelastic behavior of PVC–GCF composites was made by consideration of the main torque component  $T(\omega_1)$  and the third relative harmonic torque component  $T(3/1)$  versus the  $\gamma$  amplitude.

FT rheometry was very accurate and sensitive to material homogeneity. For instance, both  $T(\omega_1)$  and  $T(3/1)$  demonstrated that dry blending plus mixing was by far the best preparation method for PVC–GCF materials. When samples were prepared with dry blending plus extrusion, a large scatter was observed in FT rheometry results that likely reflected a poor plasticization of the PVC matrix. An easy extrapolation method gave access to linear  $G^*$  data, even when no linear behavior was reached within the  $\gamma$  window of the instrument, quite a typical observation with highly filled polymer systems. The so-derived dynamic  $G_0^*$  data suggest that the reinforcing effect of GCF loading in composites was at best hydrodynamic, with little or no polymer–fiber interfacial interactions. In addition, differences in nonlinear behavior, due to the growing fiber level, were easily and clearly detected, and the dependence on  $\gamma$  of the relative third harmonic component was adequately modeled with a simple three-parameter model. This models allowed single numbers to be extracted from the experimental data, which expressed in a very convenient manner the effect of fiber loading.

**APPENDIX A**  
**RPA-FT (1 Hz and 100°C) Main Signal Components (au) and FT Rheometry Results of 8192**  
**Data Points at 512 Points/s (16 Cycles): Test a**

$\gamma$		Samples prepared by dry blending plus extrusion						Samples prepared by dry blending plus internal mixing					
		VCF00e2		VCF80e2		VCF70e2		VCF00mi		VCF80mi		VCF70mi	
%	°	Torque	$\gamma$	Torque	$\gamma$	Torque	$\gamma$	Torque	$\gamma$	Torque	$\gamma$	Torque	$\gamma$
Run 1													
6.98	0.50	173.60	22.30	243.20	22.42	460.10	22.39	169.30	22.46	272.10	22.32	382.70	22.43
13.96	1.00	344.70	45.34	381.30	45.32	730.10	45.19	338.30	45.25	487.90	45.30	644.10	45.35
34.91	2.50	786.50	113.90	645.20	113.80	1206.00	113.70	786.90	113.70	929.00	113.70	1125.00	113.60
69.81	5.00	1286.00	227.60	924.90	227.50	1625.00	227.50	1297.00	227.40	1357.00	227.50	1533.00	227.50
118.68	8.50	1686.00	387.10	1219.00	387.00	1960.00	386.80	1627.00	387.10	1629.00	387.00	1840.00	387.10
167.55	12.00	1861.00	546.70	1473.00	546.70	2164.00	546.60	1747.00	546.60	1768.00	546.60	1952.00	546.80
237.36	17.00	1940.00	774.30	1702.00	774.30	2302.00	774.20	1819.00	774.10	1861.00	774.10	2014.00	774.50
314.16	22.50	1962.00	1025.00	1786.00	1025.00	2267.00	1025.00	1827.00	1025.00	1868.00	1025.00	2001.00	1025.00
383.97	27.50	1871.00	1253.00	1730.00	1253.00	2125.00	1253.00	1792.00	1253.00	1816.00	1253.00	1929.00	1253.00
439.82	31.50	1820.00	1435.00	1680.00	1435.00	2025.00	1435.00	1771.00	1435.00	1772.00	1435.00	1869.00	1435.00
Run 2													
8.38	0.60	188.20	27.02	285.50	27.12	393.10	27.13	189.20	27.10	276.80	27.06	355.90	27.13
20.94	1.50	450.10	68.15	572.10	68.13	758.40	68.15	461.00	68.05	603.30	68.14	706.80	68.18
48.87	3.50	914.90	159.40	962.40	159.40	1201.00	159.30	947.90	159.30	1049.00	159.40	1107.00	159.40
93.55	6.70	1332.00	305.00	1277.00	304.90	1541.00	305.10	1381.00	305.10	1355.00	305.00	1390.00	304.90
139.63	10.00	1524.00	455.60	1441.00	455.70	1696.00	455.70	1526.00	455.60	1470.00	455.80	1546.00	455.50
202.46	14.50	1638.00	660.30	1570.00	660.60	1841.00	660.60	1628.00	660.50	1598.00	660.60	1674.00	660.30
279.25	20.00	1743.00	911.10	1648.00	911.10	1898.00	911.30	1702.00	911.30	1663.00	911.30	1744.00	910.90
349.07	25.00	1784.00	1139.00	1681.00	1139.00	1895.00	1139.00	1745.00	1139.00	1691.00	1139.00	1765.00	1139.00
418.88	30.00	1785.00	1367.00	1691.00	1367.00	1876.00	1367.00	1758.00	1367.00	1701.00	1367.00	1766.00	1366.00
460.77	33.00	1775.00	1503.00	1684.00	1503.00	1851.00	1503.00	1755.00	1504.00	1694.00	1503.00	1752.00	1503.00

**APPENDIX B**  
**RPA-FT (1 Hz and 100°C) Main Signal Components (au) and FT Rheometry Results of 8192**  
**Data Points at 512 Points/s (16 Cycles): Test b**

$\gamma$		Samples prepared by dry blending plus extrusion						Samples prepared by dry blending plus internal mixing					
		VCF00e2		VCF80e2		VCF70e2		VCF00mi		VCF80mi		VCF70mi	
%	°	Torque	$\gamma$	Torque	$\gamma$	Torque	$\gamma$	Torque	$\gamma$	Torque	$\gamma$	Torque	$\gamma$
Run 1													
8.38	0.60	189.80	26.90	338.70	26.96	521.40	26.93	194.30	27.00	337.40	26.97	429.20	26.99
20.94	1.50	467.00	68.17	696.10	68.10	944.30	68.09	477.00	68.05	702.60	68.03	831.00	68.04
48.87	3.50	961.90	159.40	1181.00	159.30	1454.00	159.40	995.40	159.30	1210.00	159.50	1296.00	159.40
93.55	6.70	1414.00	305.00	1624.00	304.90	1844.00	305.10	1445.00	305.00	1581.00	305.10	1673.00	305.00
139.63	10.00	1653.00	455.50	1894.00	455.50	2055.00	455.60	1665.00	455.60	1787.00	455.60	1865.00	455.40
202.46	14.50	1817.00	660.30	2038.00	660.40	2198.00	660.50	1768.00	660.50	1878.00	660.60	1965.00	660.40
279.25	20.00	1900.00	910.90	2051.00	910.90	2216.00	911.10	1829.00	911.00	1893.00	911.20	1987.00	911.00
349.07	25.00	1878.00	1139.00	1966.00	1139.00	2103.00	1139.00	1832.00	1139.00	1840.00	1139.00	1933.00	1139.00
418.88	30.00	1802.00	1366.00	1866.00	1366.00	1971.00	1366.00	1796.00	1366.00	1787.00	1366.00	1863.00	1366.00
460.77	33.00	1751.00	1503.00	1813.00	1503.00	1885.00	1503.00	1772.00	1503.00	1749.00	1503.00	1816.00	1503.00
Run 2													
6.98	0.50	69.05	22.59	242.40	22.50	314.00	22.50	157.40	22.53	236.00	22.55	295.30	22.58
13.96	1.00	133.90	45.32	448.80	45.37	538.70	45.32	313.50	45.31	436.80	45.31	516.80	45.30
34.91	2.50	310.50	113.80	893.60	113.70	970.10	113.80	730.40	113.80	862.60	113.80	923.50	113.80
69.81	5.00	548.70	227.70	1270.00	227.50	1300.00	227.40	1206.00	227.70	1233.00	227.70	1244.00	227.60
118.68	8.50	789.20	386.80	1482.00	387.10	1527.00	386.90	1477.00	387.20	1412.00	387.00	1448.00	387.10
167.55	12.00	959.00	546.50	1611.00	546.80	1650.00	546.60	1588.00	546.80	1525.00	546.60	1580.00	546.80
237.36	17.00	1129.00	774.00	1694.00	774.40	1724.00	774.10	1666.00	774.40	1619.00	774.20	1672.00	774.20
314.16	22.50	1270.00	1025.00	1733.00	1025.00	1758.00	1025.00	1725.00	1025.00	1669.00	1024.00	1720.00	1025.00
383.97	27.50	1386.00	1252.00	1746.00	1253.00	1762.00	1252.00	1752.00	1253.00	1690.00	1252.00	1735.00	1253.00
439.82	31.50	1463.00	1434.00	1743.00	1435.00	1747.00	1435.00	1759.00	1435.00	1694.00	1435.00	1729.00	1435.00

**APPENDIX C**  
**RPA-FT (1 Hz and 100°C) Relative Third Harmonic Components (%) and FT Rheometry Results**  
**of 8192 Data Points at 512 Points/s (16 Cycles): Test a**

$\gamma$		Samples prepared by dry blending plus extrusion						Samples prepared by dry blending plus internal mixing					
		VCF00e2		VCF80e2		VCF70e2		VCF00mi		VCF80mi		VCF70mi	
		T(3/1)	S(3/1)	T(3/1)	S(3/1)	T(3/1)	S(3/1)	T(3/1)	S(3/1)	T(3/1)	S(3/1)	T(3/1)	S(3/1)
%	°												
<b>Run 1</b>													
6.98	0.50	1.37	0.85	3.37	2.06	2.02	1.68	2.56	1.75	1.85	1.27	2.06	1.64
13.96	1.00	1.72	1.00	4.69	1.84	3.03	2.26	3.06	2.18	2.61	1.71	2.56	1.72
34.91	2.50	2.37	1.18	6.38	1.98	4.89	1.92	2.59	1.78	3.94	1.67	4.20	1.83
69.81	5.00	3.09	1.12	8.19	1.59	6.63	1.65	3.01	1.38	5.25	1.41	6.48	1.50
118.68	8.50	3.60	0.70	9.12	1.01	8.84	1.13	3.96	0.92	7.51	0.95	9.20	1.10
167.55	12.00	5.50	0.55	10.07	0.74	10.60	0.89	6.29	0.69	9.37	0.74	11.00	0.87
237.36	17.00	8.30	0.48	11.02	0.62	11.98	0.71	9.25	0.56	11.00	0.60	12.53	0.68
314.16	22.50	10.09	0.43	11.87	0.52	13.11	0.59	11.17	0.47	12.44	0.51	13.89	0.55
383.97	27.50	11.23	0.38	12.93	0.45	14.16	0.51	12.20	0.42	13.71	0.46	14.99	0.47
439.82	31.50	12.16	0.38	13.84	0.43	15.02	0.47	12.93	0.40	14.65	0.44	15.73	0.44
<b>Run 2</b>													
8.38	0.60	2.80	1.69	2.78	1.86	2.20	1.63	2.68	1.71	2.24	1.58	2.48	1.97
20.94	1.50	2.87	1.60	4.32	2.18	3.48	2.29	2.80	1.76	2.69	1.81	2.75	1.86
48.87	3.50	3.48	1.55	5.11	1.77	4.62	1.81	2.83	1.48	3.47	1.68	4.07	1.66
93.55	6.70	3.91	1.05	6.22	1.20	7.37	1.28	3.47	1.12	5.60	1.22	7.31	1.22
139.63	10.00	5.44	0.76	8.41	0.92	9.78	0.94	5.19	0.81	8.40	0.91	9.80	0.90
202.46	14.50	8.23	0.56	10.18	0.68	11.40	0.73	8.15	0.62	10.46	0.71	11.58	0.67
279.25	20.00	10.46	0.49	11.76	0.55	12.94	0.61	10.75	0.51	12.22	0.58	13.42	0.56
349.07	25.00	11.43	0.44	13.02	0.47	14.17	0.51	11.86	0.44	13.57	0.48	14.68	0.48
418.88	30.00	12.44	0.41	13.99	0.42	15.19	0.45	12.82	0.40	14.59	0.44	15.65	0.45
460.77	33.00	13.08	0.41	14.59	0.39	15.76	0.42	13.42	0.38	15.16	0.41	16.18	0.43

**APPENDIX D**  
**RPA-FT (1 Hz and 100°C) Relative Third Harmonic Components (%) and FT Rheometry Results**  
**of 8192 Data Points at 512 Points/s (16 Cycles): Test b**

$\gamma$		Samples prepared by dry blending plus extrusion						Samples prepared by dry blending plus internal mixing					
		VCF00e2		VCF80e2		VCF70e2		VCF00mi		VCF80mi		VCF70mi	
		T(3/1)	S(3/1)	T(3/1)	S(3/1)	T(3/1)	S(3/1)	T(3/1)	S(3/1)	T(3/1)	S(3/1)	T(3/1)	S(3/1)
%	°												
<b>Run 1</b>													
8.38	0.60	2.29	1.75	2.07	1.70	1.60	1.67	2.67	2.09	2.26	1.84	1.71	1.48
20.94	1.50	2.55	1.79	3.58	2.34	3.85	2.23	2.92	2.12	3.25	1.94	3.21	1.93
48.87	3.50	2.79	1.62	4.85	1.71	5.46	1.80	2.64	1.61	4.20	1.63	4.79	1.60
93.55	6.70	3.42	1.08	6.08	1.12	7.74	1.24	3.24	1.08	6.27	1.15	7.58	1.20
139.63	10.00	4.96	0.83	7.77	0.86	9.70	0.98	4.75	0.84	8.52	0.89	9.91	0.92
202.46	14.50	7.59	0.62	9.61	0.65	11.49	0.75	7.93	0.64	10.48	0.68	11.67	0.70
279.25	20.00	9.74	0.48	11.08	0.53	12.73	0.60	10.51	0.52	11.92	0.56	13.17	0.60
349.07	25.00	10.71	0.41	12.45	0.46	13.81	0.49	11.81	0.46	13.25	0.48	14.46	0.52
418.88	30.00	11.63	0.37	13.82	0.43	14.95	0.40	12.66	0.41	14.48	0.41	15.53	0.45
460.77	33.00	12.38	0.35	14.65	0.42	15.67	0.38	13.27	0.38	15.14	0.37	16.08	0.42
<b>Run 2</b>													
6.98	0.50	3.19	1.98	2.67	1.95	2.31	1.81	3.16	1.97	2.54	1.82	3.26	2.50
13.96	1.00	3.33	1.96	2.80	2.17	2.97	2.37	2.54	1.67	2.36	1.74	2.81	2.24
34.91	2.50	3.26	1.65	2.87	1.57	3.57	1.68	2.59	1.59	2.84	1.58	3.44	1.62
69.81	5.00	3.63	1.32	4.21	1.45	5.56	1.48	2.92	1.29	4.02	1.36	5.53	1.39
118.68	8.50	4.62	0.92	7.06	1.05	8.86	1.09	4.15	0.92	7.11	0.98	8.80	1.05
167.55	12.00	6.83	0.72	9.46	0.82	10.69	0.81	6.47	0.71	9.50	0.77	10.61	0.83
237.36	17.00	9.79	0.57	11.30	0.65	12.38	0.62	9.70	0.57	11.43	0.61	12.41	0.66
314.16	22.50	11.03	0.47	12.82	0.53	13.89	0.51	11.30	0.47	13.08	0.50	14.07	0.54
383.97	27.50	11.96	0.41	13.94	0.46	15.02	0.45	12.34	0.40	14.26	0.43	15.25	0.45
439.82	31.50	12.72	0.37	14.75	0.43	15.75	0.42	13.18	0.37	15.03	0.41	15.96	0.41

The study reported here was performed within the frame of a project sponsored by CAPES-COFECUB to promote collaboration between the University P. and M. Curie (Paris 6), France, and the Universidade Federal do Rio de Janeiro, Brazil. The author thanks Cristina R. G. Furtado and Leila Y. Visconte for drawing his attention to GCFs as a potential filler for polymers and for their assistance during the visits he made in the course of the project.

## References

1. Leblanc, J. L.; de la Chapelle, C. *Rubber Chem Technol* 2003, 76, 287.
2. Leblanc, J. L. *J Appl Polym Sci* 2003, 89, 1101.
3. Leblanc, J. L. *J Appl Polym Sci*, to appear.
4. Guth, E.; Simha, R. *Kolloid Zeitschrift* 1936, 74, 266.
5. Guth, E.; Gold, O. *Phys Rev* 1938, 53, 322.
6. Wilhelm, M. *Macromol Mater Eng* 2002, 287(2), 83.
7. Leblanc, J. L. Presented at the 9th International Seminar on Elastomers, Kyoto, Japan, April 2003.